

# Modifying the Proliferative State of Target Cells to Control DNA Expression and Identifying Cell Types Transfected *In Vivo*

Kathryn W Riddle<sup>1</sup>, Hyun-Joon Kong<sup>2</sup>, J Kent Leach<sup>2</sup>, Claudia Fischbach<sup>2</sup>, Charles Cheung<sup>3</sup>, Kristi S Anseth<sup>3</sup> and David J Mooney<sup>2</sup>

<sup>1</sup>Department of Chemical Engineering, University of Michigan, Ann Arbor, Michigan, USA; <sup>2</sup>Division of Engineering and Applied Sciences, Harvard University, Cambridge, Massachusetts, USA; <sup>3</sup>Department of Chemical and Biological Engineering, University of Colorado, Boulder, Colorado, USA

Although the majority of current gene transfer techniques have focused on increasing the ability of the DNA to enter the cell, it is possible that changing the proliferative and migratory state of cells will influence the cells ability to take up and express plasmid DNA. This study was designed to test the hypothesis that growth factors (basic fibroblast growth factor (bFGF) and hepatocyte growth factor/scatter factor (HGF/SF)) used to alter the proliferative and migratory state of cells can alter plasmid DNA uptake and expression. *In vitro* studies indicate that enhancing cell proliferation with growth factor exposure enhances plasmid DNA uptake and expression. Furthermore, dual localized delivery of bFGF and plasmid DNA *in vivo* increases the expression, 3–6 times over control, as compared to plasmid delivery alone. Dual delivery of a factor promoting cell proliferation and a plasmid led to a further increase in the expression of the plasmid encoding bone morphogenetic protein-2 in a rat cranial defect by specific cell populations. The results of these studies suggest that increasing the proliferative state of target cell populations can enhance non-viral gene transfer.

Received 16 December 2005; accepted 28 August 2006.  
doi:10.1038/sj.mt.6300017

## INTRODUCTION

Gene transfer techniques hold much promise for the treatment of disease and healing of injuries but have been limited by their safety and/or low transfer efficiencies.<sup>1</sup> Although extremely efficient, viral vectors (*i.e.* retroviruses and adenoviruses) have safety concerns in relation to immunogenicity and random incorporation into the host genome.<sup>2</sup> Non-viral vectors, including cationic polymers and lipids, have emerged as possible alternatives to viral delivery, but have been limited by low efficiency as compared to viral delivery.<sup>3,4</sup>

Although the majority of current gene transfer techniques have focused on increasing the ability of the DNA to enter the

cell, it is possible that changing the proliferative and migratory state of cells will influence their ability to take up and express plasmid DNA. It has been previously shown that cells will internalize plasmid DNA through endocytosis *in vitro*<sup>5,6</sup> and also that the amount of endocytosis will increase during migration and proliferation.<sup>7–9</sup> These findings suggest that one may increase the efficiency of gene transfer by increasing endocytosis via induced cell proliferation and migration. Growth factors are commonly utilized to promote cell proliferation and migration, and basic fibroblast growth factor (bFGF) has been shown to induce the proliferation of many cell types.<sup>10,11</sup> Hepatocyte growth factor/scatter factor (HGF/SF) can induce migration in a number of cell types.<sup>12</sup>

In light of the potential interplay between proliferation and endocytosis-mediated gene transfer, we hypothesized that growth factors used to alter the proliferative and migratory state of cells can alter plasmid DNA uptake and expression. To address this hypothesis, a combination of *in vitro* and *in vivo* studies were performed, which examined expression of both marker genes and a plasmid encoding a protein with significant therapeutic potential (bone morphogenetic protein-2 (BMP-2)), in both a subcutaneous implant site, and orthotopic wound site (cranial defect). bFGF and HGF were used as model substances to stimulate cellular proliferation and migration, respectively, in these studies.

## RESULTS

### Relation between proliferation, migration, and transfection *in vitro*

Cultured cells were exposed to varying concentrations of bFGF and HGF to confirm that their proliferation and migration could be regulated by these factors. NIH3T3 fibroblasts exhibited an increase in proliferation when exposed to bFGF concentrations of 10 ng/ml and greater (**Figure 1a**). In contrast, exposing cells to varying concentrations of HGF/SF led to no significant increase in proliferation over control conditions (**Figure 1b**). Cells were then exposed to 'high' (50 ng/ml) or 'low' (10 ng/ml) concentrations of bFGF and HGF to determine if migration was influenced

Correspondence: David J Mooney, Division of Engineering and Applied Sciences, Harvard University, 29 Oxford Street, 325 Pierce Hall, Cambridge, Massachusetts 02138, USA. E-mail: mooneyd@deas.harvard.edu

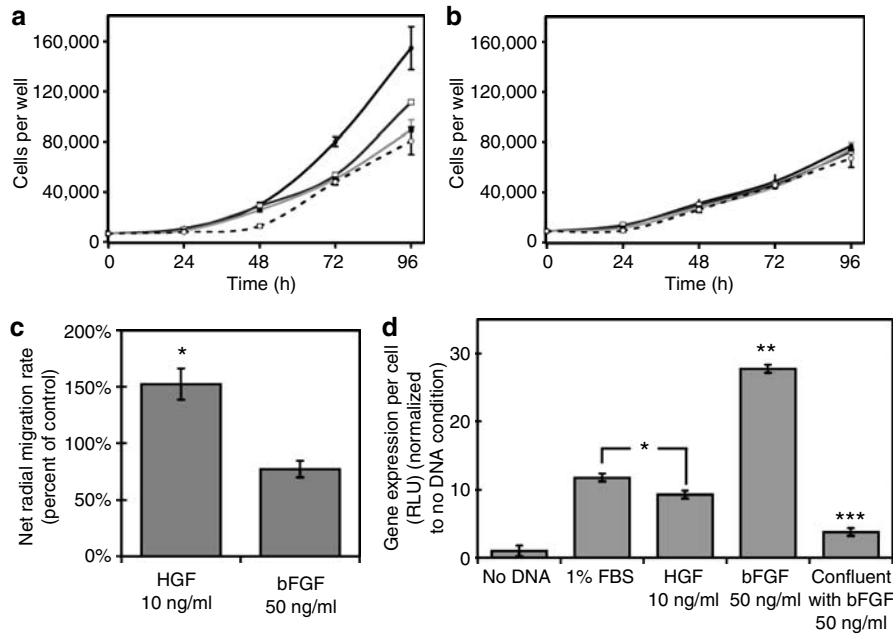


**Figure 1** *In vitro* characterization of the growth factors. Quantification of the change in NIH3T3 fibroblast cell number in response to 1% FBS-containing media supplemented with 50 ng/ml (●), 10 ng/ml (□), 1 ng/ml (■), and 0 ng/ml (○) (a) bFGF or (b) HGF/SF. (c) Net radial migration as a percentage of control (1% FBS). Values represent mean ( $n=6$ ) and SD. \*Significance with  $P<0.005$ . (d) Expression of  $\beta$ -gal was analyzed as a quantitative measure of NIH3T3 transfection in the presence of HGF and bFGF. Relative light units (RLU) were measured and normalized to the control where no DNA was delivered. Values represent mean ( $n=4$ ) and SD. \*Significance between data points with  $P<0.003$ , and \*\*significance over all other data points with  $P<0.001$ . In addition, \*\*\*significance over "No DNA" condition with  $P<0.01$ .

by these growth factors. Neither concentration of bFGF caused significant increases in migration. In contrast, low concentrations of HGF caused a significant increase in migration in NIH3T3 fibroblasts (Figure 1c).

Cells were subsequently transfected in the presence of these growth factors to assess if they increased transfection (Figure 1d). Exposure of cells to bFGF led to a significant increase in the gene expression level, as compared to control medium. In contrast, gene expression levels were not enhanced when cells were cultured with HGF. To rule out the possibility that the bFGF was increasing DNA expression through means other than proliferation, cells were transfected in the presence of bFGF when cultured in a confluent state that inhibited proliferation. These cells had significantly decreased levels of gene expression.

To determine if cell transfection correlated directly with the proliferation of individual cells, cells that were transfected with green fluorescent protein (GFP) were also immunostained for the presence of proliferating cell nuclear antigen (PCNA), and co-localization of the two fluorescent probes was assessed. PCNA immunohistochemistry positively stains the nuclei of cells that have recently passed through the S phase of the cell cycle, and therefore provides a marker of recent cell proliferation. Fluorescent images of transfected cell demonstrated significant co-localization of PCNA with GFP expression (Figure 2a). While 52% of the cells in this population were proliferating, approximately 31% of the cells were transfected with GFP. However, 98% of the transfected cells also had positive PCNA staining, indicating that cells which are actively proliferating are largely responsible for plasmid expression. To determine, whether the increase in cell proliferation was increasing plasmid

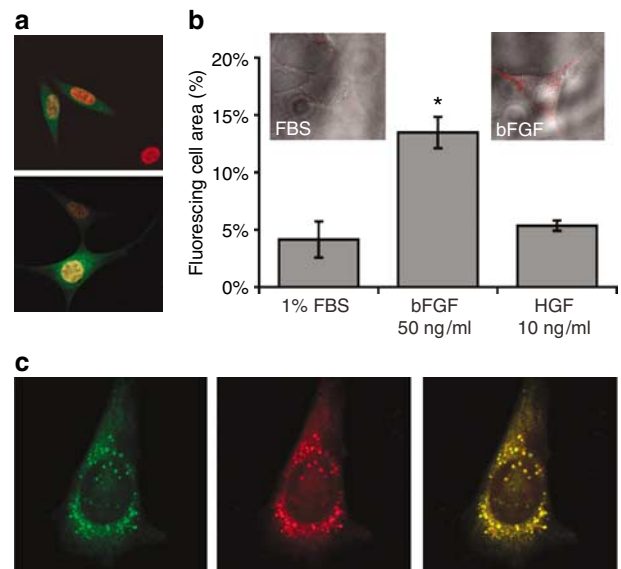


**Figure 2** Mechanism of DNA Uptake. (a) Representative confocal photomicrographs showing co-localization of GFP-transfected (green) cells and the PCNA (red). (b) Fluorescing cell area as a qualitative measure of the amount of labeled PEI/DNA condensates within the cells. Values represent mean ( $n=25$ ) and SD. \*Significance over other data points with  $P<0.004$ . (c) Representative photomicrographs showing co-localization (yellow) of the lysotracker dye (green) and the PEI/DNA condensates (red).

DNA uptake as well as expression, fluorescent polyethylenimine (PEI)/DNA condensates were prepared, exposed to cells, and the internalized PEI/DNA condensates were visualized with confocal microscopy under varying degrees of proliferative stimuli.

Qualitative analysis suggested a significant increase in DNA uptake when the cells were cultured in conditions promoting proliferation (Figure 2b). To confirm the mechanism of DNA uptake into these cells, a dye that localizes to lysosomes was used to track cellular internalization of DNA (Figure 2c). Cells were transfected with PEI/DNA condensates, allowed to incubate overnight, and exposed to media containing the lysotracker dye. Visual analysis of over 100 cells demonstrated a strong colocalization of the DNA and the lysotracker dye within cells, indicating that the mechanism of PEI/DNA condensate uptake was endocytosis, and that endocytotic uptake of PEI/DNA was increased in proliferating cell populations.

### Gene expression and cell infiltration *in vivo*

To determine if increasing cell proliferation and/or migration could similarly enhance gene uptake *in vivo*, polymeric scaffolds releasing plasmid DNA with or without simultaneous bFGF release were fabricated and implanted into two animal models. Scaffolds were formed from microspheres (Figure 3a), and possessed an interconnected porous structure (Figure 3b) that has been previously demonstrated to support host cell infiltra-

tion.<sup>13,14</sup> The efficiency of bFGF incorporation into the scaffolds was  $79 \pm 5\%$ . *In vitro*, 50% of the incorporated bFGF was released in the first 5 days when scaffolds were placed in an aqueous environment, followed by approximately 1% per day for the duration of the study (Figure 3c). The efficiency of plasmid DNA incorporation into scaffolds was  $61 \pm 3\%$ . Immersion of scaffolds in aqueous medium *in vitro* led to a release of 50% of the DNA in the first 4 days, followed by a release rate of 0.4% per day for the duration of the study (Figure 3c). To confirm that the bFGF retained biological activity after incorporation and release, the released bFGF was added to cultured cells, and their proliferation was monitored. Knowledge of the release kinetics of bFGF from these scaffolds, together with the known response of NIH3T3 cells to various concentrations of bFGF, allowed the calculation of released bioactivity to be 80–100% of initial bioactivity over a 42-day release period *in vitro* (Figure 3d).

Scaffolds containing the  $\beta$ -galactosidase ( $\beta$ -gal) plasmid were implanted into the subcutaneous tissue of Lewis rats, and subsequently removed after 2, 4, and 8 weeks to determine if plasmid expression was increased with simultaneous bFGF delivery. At all time points, scaffolds releasing plasmid DNA in

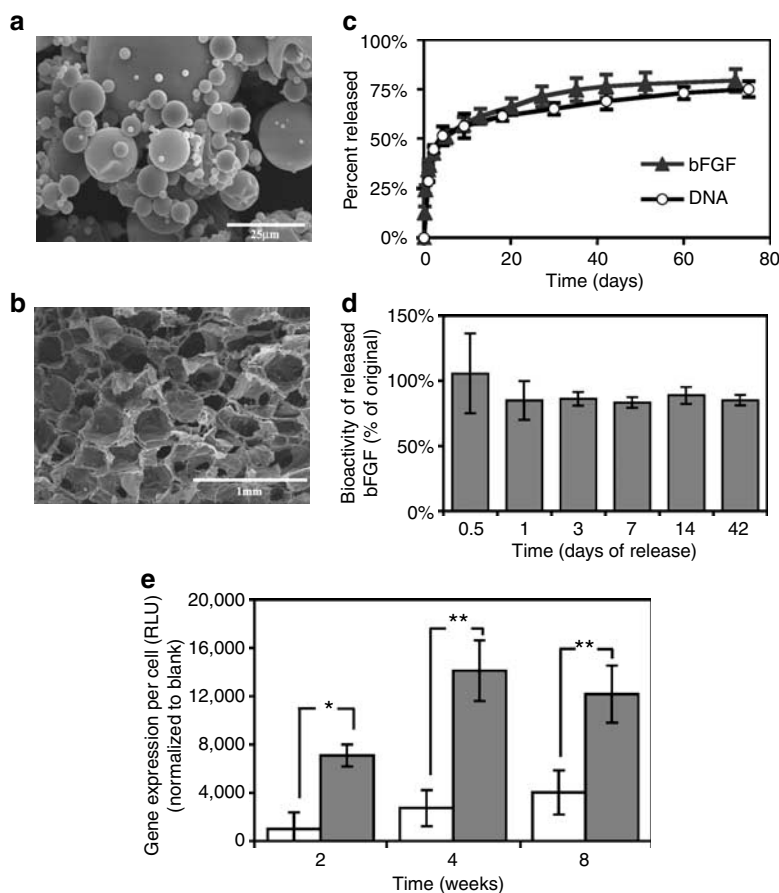


**Figure 3** Scaffold characterization and subcutaneous gene expression. Photomicrographs of (a) PLG microspheres used to fabricate (b) gas-foamed scaffolds. *In vitro* release profile of bFGF (c, ▼) and plasmid DNA (c, ○) from PLG scaffolds. Values represent mean ( $n=6$ ) and SD. (d) Bioactivity of released bFGF, relative to bFGF never incorporated into scaffolds. Values represent mean ( $n=6$ ) and SD. (e)  $\beta$ -gal expression at 2, 4, and 8 weeks following implantation with (■) or without (□) simultaneous growth factor ( $3 \mu\text{g}$  bFGF) delivery. Values represent mean ( $n=4$ ) and SD. \*Significance with  $P < 0.025$  and \*\* $P < 0.01$ .

conjunction with bFGF showed significantly enhanced gene expression, as compared to scaffolds releasing DNA alone (Figure 3e). Gene expression appeared to peak at week 4, with a 5-fold increase in gene expression when bFGF was co-delivered, as compared to the condition without bFGF delivery. In addition to gene expression, angiogenesis was quantified at 2 and 4 weeks and it was shown that the blood vessel density within the tissue infiltrating the scaffolds increased 1.7-fold over the control when bFGF was delivered but no increase was seen with DNA delivery alone (Figure 4). The number and types of cells migrating into scaffolds in response to varying amounts of bFGF was next quantified to confirm that the locally released bFGF altered the number of cells present in the scaffolds which could be potentially capable of taking up and expressing the plasmid. There was a dose-dependent increase in the density of cells with the bFGF concentration (Figure 5a), and the effect was most pronounced as the dose was raised from 0.5 to 3 µg bFGF per scaffold. This effect leveled off at 10 µg bFGF. Analysis of the cell types entering the scaffold was performed using fluorescence-activated cell sorting on cells isolated from the scaffolds following explantation. Isolated cells were stained for cell surface markers for endothelial cells (CD31: also has low-level expression on platelets, macrophages, and monocytes) and lymphocytes (CD45). Although the cellular density was increased with increasing bFGF concentrations, the composition of the invading tissue was statistically indistinguishable with or without bFGF delivery (Figure 5b). The unidentified cell population (termed 'Other') in these populations appeared to be mostly fibroblasts, as based on their morphology in tissue sections stained with hematoxylin and eosin. The increase in the density of blood vessels in the condition in which bFGF was delivered, was consistent in magnitude with the increase in endothelial cells in these tissues. In all conditions, approximately 28% of the cells invading scaffolds were CD31-positive, 25% were CD45-positive, and the remaining 47% were fibroblasts.

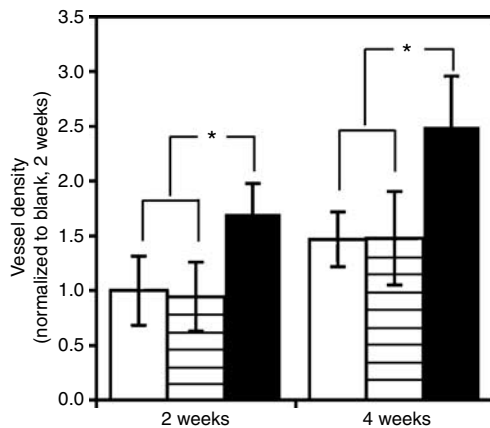


Figure 4 Angiogenesis with bFGF and pDNA delivery. Quantification of blood vessel density in the tissues, relative to the blood vessel density in blank scaffolds at 2 weeks. White bars represent blank scaffolds, striped bars represent scaffolds releasing plasmid DNA (encoding for β-gal), and black bars represent scaffolds releasing plasmid DNA and growth factor (bFGF, 3 µg). Values represent mean (n=4) and SD where \*significance with P<0.02.

The ability of this approach to enhance the expression of a therapeutic protein in a model more relevant to tissue engineering was then assessed after 3, 8, and 15 weeks by delivery of a gene encoding BMP-2 into a cranial defect in rats. Importantly, the expression of the BMP-2 plasmid was again increased with simultaneous bFGF delivery (Figure 6), similar to

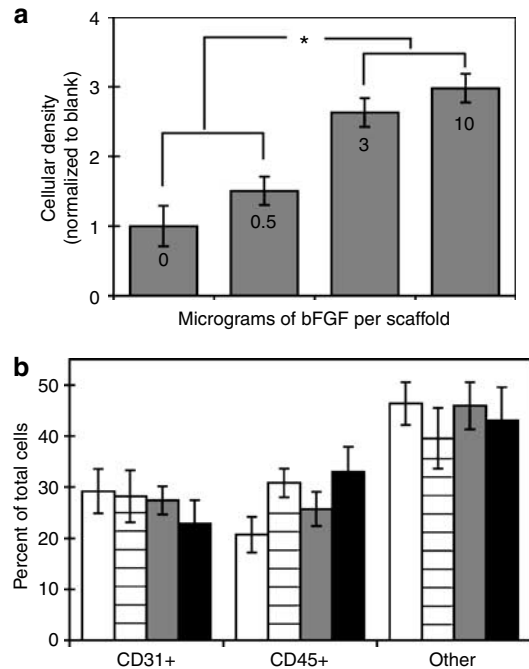


Figure 5 *In vivo* subcutaneous response to bFGF. (a) Cellular densities in PLG scaffolds at 1 week post-implantation as a function of the amount of bFGF in the scaffolds. Values represent mean (n=4) and SD. \*Significance with P<0.02 and \*\*P<0.002. (b) Composition, in percent, of each cell population infiltrating the PLG scaffolds at 1 week post-implantation. 0 µg bFGF (white bars), 0.5 µg bFGF (striped bars), 3 µg bFGF (gray bars), and 10 µg (black bars) bFGF were delivered. Values represent mean (n=4) and SD, with no statistically significant differences between the conditions.

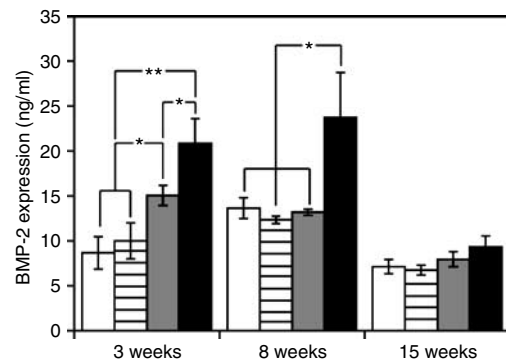
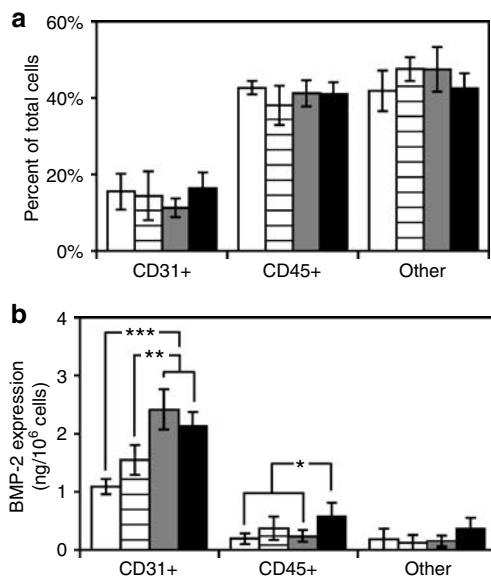


Figure 6 BMP-2 expression in the cranial defect. Quantification of BMP-2 expression in the cranial defect at 3 (n=4), 8 (n=5), and 15 (n=6) weeks. All scaffolds contained plasmid DNA, with white and striped bars representing conditions using DNA encoding for GFP, whereas gray and black bars represent DNA encoding for BMP-2. Striped and black bars represent scaffolds that also contained bFGF (3 µg). Values represent the mean and SD where \*significance with P<0.02, and \*\* with P<0.002.



**Figure 7** *In vivo* cranial defect. Response to bFGF and DNA delivery. **(a)** Cellular composition of the tissue forming in the scaffolds implanted into cranial defect (3 weeks post-implantation). All scaffolds contained plasmid DNA, with white and striped bars representing conditions using DNA encoding for GFP, whereas gray and black bars represent DNA encoding for BMP-2. Striped and black bars represent scaffolds that also contained bFGF (3  $\mu$ g). Values represent mean ( $n=4$ ) and SD, and no statistically significant differences were noted between conditions. **(b)** BMP-2 expression in the various cell populations within the scaffolds at 3 weeks post-implantation. All scaffolds contained plasmid DNA, with white and striped bars representing conditions using DNA encoding for GFP, whereas gray and black bars represent DNA encoding for BMP-2. Striped and black bars represent scaffolds that also contained bFGF (3  $\mu$ g). Values represent mean ( $n=4$ ) and SD. \*\*\*Statistical significance with  $P<0.002$ , \*\* $P<0.02$ , and \* $P<0.05$ .

the results from the subcutaneous implant study. Magnetic-assisted cell sorting was performed to determine the composition of the cells invading the scaffold (**Figure 7a**). Similar to the subcutaneous studies performed, the composition of the invading tissue (percentage of each cell type) did not change regardless of whether the growth factor (bFGF) was delivered. Lysing of the different cell populations indicated that the CD31-positive cell population had the highest baseline expression of BMP-2, but the increase in gene expression with bFGF delivery was related to enhanced expression in both this population and the CD45-positive cell population (**Figure 7b**).

## DISCUSSION

The results of these studies suggest that increasing the proliferative state of target cell populations, which can also potentially be accomplished via a variety of material cues (e.g., growth factors, modulation of matrix properties, and small molecule drugs), can enhance non-viral gene transfer. *In vitro* studies indicate that enhancing cell proliferation with growth factor exposure enhances plasmid DNA uptake and expression. Furthermore, dual localized delivery of bFGF and plasmid DNA *in vivo* increases the expression of the factor encoded by the plasmid. In addition, although CD31-positive cells are mainly responsible for expression of a plasmid delivered to a cranial

defect, the addition of a proliferative factor such as bFGF also causes an increase in expression in CD45-positive cells.

Stimulating cell proliferation enhanced gene transfer *in vitro*. Exposure of cells to bFGF, which greatly enhanced proliferation, significantly increased transfection efficiency. In contrast, exposure of cells to a migratory stimuli (10 ng/ml HGF/SF) led to a slight decrease in DNA expression. Further, exposure of cells to bFGF when proliferation was contact inhibited did not lead to increased transfection. The tight correlation between passage through the cell cycle and uptake and expression of the gene encoded by the plasmid also supports the conclusion that enhancing proliferation was key to improving transfection in these studies. This observation extends and supports the previous finding that plasmid DNA delivered using cationic liposomes was most likely to enter the cell during mitosis.<sup>9</sup> More recently, the demonstration that the stiffness of the substrate to which cells are adherent impacts cell transfection levels, provides another approach to exploit the dependency of gene transfer on the proliferative state of the targeted cell population.<sup>15</sup> Although an alternate explanation for our findings is that bFGF complexed with DNA to form condensates that enhanced uptake and expression, the concentration of bFGF used in our process is significantly below that which has been reported to be required for the bFGF to have a significant condensing effect.<sup>16</sup>

Dual presentation of bFGF and DNA enhanced DNA expression *in vivo* by a factor of 3–6 over the 8-week time period studied in these experiments. Uncomplexed DNA has been shown by other researchers to enter the cell and be expressed with varying amounts of success.<sup>17–19</sup> However, large amounts (up to 1 mg) of plasmid DNA have typically been required to obtain the desired level of expression. The results of this study indicate that increasing the density and proliferation of cells at the delivery site allows one to obtain a significant level gene expression even with smaller quantities of plasmid DNA. The cellular density at the delivery site increased 2–3 times with the delivery of bFGF, and this is likely a result of both enhanced recruitment of host cells and increased proliferation of the recruited cells. The increase in cell number alone may partially explain the increased gene expression. However, the increase in gene expression was much greater than the overall increase in cell number, implying that a change in cell behavior, presumably increased passage through the cell cycle, also contributed to the increase in gene expression. No direct analysis of proliferation *in vivo* was performed in these experiments, but previous studies have demonstrated that local delivery of bFGF does cause an increase in the number of cells proliferating at the site.<sup>20</sup>

Analysis of the cells entering the scaffolds used to deliver the plasmid DNA and growth factors revealed that the CD31-positive cell population exhibits the greatest level of transfection. It has previously been shown that CD31-positive cells synthesize BMP-2,<sup>21</sup> so it is not surprising that these cells exhibited high basal levels of BMP-2 expression in our studies. It is surprising, however, that these cells were a major factor in expression of the delivered plasmid DNA. In addition, the CD45-positive cell population, while exhibiting lower overall levels of gene expression, demonstrated a significant increase in expression with bFGF co-delivery. Although co-delivery of bFGF and pDNA

increased BMP-2 expression, the addition of bFGF in a cranial defect could complicate osteogenesis studies, as bFGF has been shown to play a role in osteogenesis.<sup>22-24</sup> Previous studies have identified the cell populations taking up and expressing plasmid DNA delivered with polymeric depots based only on morphological analysis of tissue sections.<sup>14,19</sup> The analysis presented in this report represents the first specific analysis of the cell types expressing plasmid DNA delivered from a polymeric depot, and knowledge of the cell types participating in expression of the delivered plasmid could enable one to choose growth factors to specifically recruit desired cell populations for specific applications in the future. Additional studies will be required to determine if enhanced BMP-2 expression obtained with bFGF delivery leads to an increase in osteogenesis, and these studies will also have to consider the potential effects of bFGF itself on bone regeneration. Delivery of bFGF has been reported to both enhance<sup>25-27</sup> and to inhibit<sup>24,28</sup> bone regeneration in other studies.

This paper demonstrates that one can modify cellular behavior *in vivo* using growth factors to increase the expression of plasmid DNA delivered from polymeric depots. Previous studies have shown that plasmid DNA, delivered from poly(lactide-co-glycolide) (PLG) scaffolds, affects cells in close proximity to the implanted scaffold.<sup>17</sup> This finding, along with the very short serum half-life of DNA *in vivo* (4–30 min<sup>29,30</sup>), implies that plasmid DNA does not travel very far from the delivery site before it is either taken up by the cells and/or degraded. In light of this constraint, it is clear that simultaneously encouraging host cells to migrate towards a delivery vehicle and enhancing their tendency to take up and express plasmid DNA, as demonstrated in this report, can significantly impact localized gene therapy.

## MATERIALS AND METHODS

**DNA sources.** Naked plasmid DNA and condensed DNA encoding for  $\beta$ -gal, GFP, or BMP-2 were used in these experiments. All plasmids used in these studies contained the cytomegalovirus promoter. Plasmid DNA encoding for  $\beta$ -gal or GFP was obtained from Aldevron (Fargo, ND). Plasmid DNA encoding for BMP-2 was first obtained from Christopher Evans at Brigham and Women's Hospital (Harvard University) and expanded by Aldevron. *In vitro* studies to explore the mechanism of DNA uptake were performed with condensed DNA encoding for GFP or  $\beta$ -gal. Subcutaneous *in vivo* gene transfer and expression data were obtained using plasmid DNA encoding for  $\beta$ -gal, whereas the cranial defect studies used condensed DNA encoding for BMP-2.

**Condensed DNA.** Branched PEI (MW = 25,000, Sigma-Aldrich, St Louis, MO) was used to condense plasmid DNA (gWiz™ GFP, Aldevron, Fargo, ND) for more efficient transfection in certain experiments as described previously.<sup>15</sup> In certain experiments, PEI was fluorescently labeled as described previously with carbodiimide chemistry,<sup>15</sup> and used to make PEI/DNA condensates.

**In vitro growth factor characterization.** In order to assess proliferation influenced by bFGF and HGF, NIH3T3 cells were plated (20,000 cells/ml) in Dulbecco's modified Eagle's medium overnight. Media was exchanged for 1% fetal bovine serum (FBS), 10% FBS, or conditioned media (1% FBS with bFGF or HGF/SF). Media was changed daily and proliferation was monitored by performing cell counts (Beckman Coulter, Fullerton, CA;  $n = 4$ ).

To measure overall population migration, 2,000 cells were seeded on tissue culture polystyrene dishes in 2 mm diameter circular adhesive regions. The adhesive regions were created by placing a silicon sheet, containing 2 mm diameter holes, onto the bottom of a six-well tissue culture plate before cell seeding and seeding the cells into the resultant well formed by the silicon sheet. Cells were cultured for 12 h to allow adhesion, and the silicon sheet was then removed, and cells were washed with fresh medium. Cell motility was monitored by determining the distance along the substrate in the radial direction traveled by the cell population, using an inverted microscope system with digital camera (TE300; Nikon, RT slider; Diagnostic Instruments, Sterling Heights, MI). Phase contrast images were analyzed with Spot 4.0 (Diagnostic Instruments) and Photoshop 7.0 (Adobe, San Jose, CA).

To assess the effect of the proliferation and migration on transfection efficiency *in vitro*, cells were seeded at 150,000 cells/ml in a six-well plate 24 h before transfection. Transfection of DNA (gWiz™ GFP, Aldevron, Fargo, ND) encoding for GFP was performed according to the Polyfect (Qiagen, Valencia, CA) transfection reagent protocol. In one condition, cells were plated at confluence and exposed to 50 ng/ml bFGF during transfection. Fluorescent images were taken, and cells were counted using a Beckman coulter counter and measured for total fluorescence on a Tecan GENios<sup>®</sup> fluorometer (excitation 488 nm, emission 535 nm, and 1 s integration). When PEI condensed DNA was used in the transfection studies, 20  $\mu$ l of condensate solution was pipetted over a 50% confluent well of an eight-well culture slide. Condensates were allowed to incubate with the cells for 12 h before imaging with a confocal microscope (LSM5 Pascal, Zeiss, Thornwood, NY).

**Intracellular staining for PCNA, GFP, and lysosomes.** Cells transfected with condensed DNA (gWiz™ GFP, Aldevron, Fargo, ND) or DNA/Polyfect condensates for 12 and 24 h were fixed with 4% paraformaldehyde and subsequently stained for GFP activity and/or PCNA. In brief, cells were washed with phosphate-buffered saline (PBS), exposed to a boiling solution of 10 mM tri-sodium citrate and 0.5 ml Tween 20 in distilled water at pH 6.0, and following a subsequent wash with PBS, placed in a blocking solution (10% normal goat serum, 2% bovine serum albumin, 0.25% Triton X). Slides were then exposed to primary polyclonal antibody for GFP conjugated to AlexaFluor488 (Molecular Probes; Eugene, OR) and a monoclonal antibody for PCNA (Zymed Laboratories Inc., San Francisco, CA) diluted in the blocking solution at 1:1,000 and 1:2,000, respectively. Another wash with PBS was followed by incubation with the secondary antibody to PCNA (goat anti-mouse immunoglobulin G Cy5) at a concentration of 1:200. Subsequently, cells were imaged using Zeiss LSM 5 Pascal (Thornwood, NY) confocal microscope at excitation wavelengths of 488 and 633 nm and emission wavelengths of 520 and 690 nm, respectively. The percentage of the cell containing fluorescing condensates was determined using NIH ImageJ software. The area of the fluorescence was first determined using threshold counting. Subsequently, the total area of the cell was determined using the freehand selection and measurement feature. In order to identify if the PEI/DNA condensates were entering the cell via endocytosis, a LysoTracker dye was used to stain lysosomal components in cultured cells. LysoTracker dye was used and imaged according to the protocol from Invitrogen (Carlsbad, CA). Rhodamine-PEI condensates were imaged at an absorbance of 560 nm and emission of 620 nm.

**Scaffold fabrication and characterization.** Microspheres were fabricated from 75:25 PLG (inherent viscosity 0.76, MW 113 kDa, Alkermes, Cincinnati, OH) with a water/oil/water double emulsion process.<sup>31</sup> Scaffolds were fabricated from microspheres as described previously.<sup>32,33</sup> For scaffolds containing growth factors (bFGF, National Cancer Institute) and/or plasmid DNA (gWiz™ Beta-gal, Aldevron, Fargo, ND), slight modifications to the process were made. bFGF was

incorporated by mixing a solution of 1% alginate and the appropriate amount of growth factor (0.1  $\mu\text{g}/\mu\text{l}$  bFGF in  $\text{dH}_2\text{O}$ ) with the polymer microspheres and lyophilizing before adding the poragen. DNA was incorporated by using DNA-loaded microspheres as the base material in the gas-foaming process. These approaches yielded scaffolds with approximately 200  $\mu\text{g}$  of plasmid DNA, and either 0.5, 3, or 10  $\mu\text{g}$  bFGF.

To determine the incorporation efficiency and release kinetics of bFGF from the porous scaffolds,  $^{125}\text{I}$ -labeled human recombinant bFGF (195  $\mu\text{Ci}/\mu\text{g}$ ) (Perkin-Elmer; Boston, MA) was utilized as a tracer and was performed as described previously.<sup>34</sup> Bioactivity of released bFGF was analyzed by performing a proliferation assay with NIH3T3 cells using non-radioactive bFGF released at varying time points as described previously.<sup>35</sup>

To determine the release rate of plasmid DNA from porous PLG scaffolds, scaffolds were placed in 2 ml of PBS and maintained at 37°C. At various time points, the PBS was removed and a dye-binding assay was performed (Hoechst 33258 dye, Molecular Probes; Eugene, OR).

**Scaffold implantation.** All animal studies were conducted under guidelines set forth by the Institutional Animal Care and Use Committee at University of Michigan and Harvard University. Scaffolds were implanted subcutaneously in the dorsal area of Lewis rats (male, 7–9 weeks old) for periods of 1 and 2 weeks to assess tissue ingrowth as described previously.<sup>36</sup> Sections of the implanted scaffolds were subsequently stained with hematoxylin and eosin for further analysis. Rat cranial defect studies were performed in accordance with the Harvard University animal care guidelines, and all NIH animal handling procedures were observed. Cranial defect surgeries were performed as described previously.<sup>37</sup> Scaffolds containing condensed DNA (encoding for either GFP or BMP-2) with or without bFGF were placed in the critical sized defect site. After 3, 8, and 15 weeks, animals were killed with carbon dioxide and the implants along with surrounding bone were retrieved. A 2 mm diameter biopsy of the implant was removed to perform biochemical analysis and the rest of the scaffold was fixed for 24 h in 4% paraformaldehyde at 4°C.

**Determination of cellular infiltration and angiogenesis.** Cells that had infiltrated PLG scaffolds at 1 week following subcutaneous implantation were isolated by exposing retrieved scaffolds to 200 U/ml type 2 collagenase (Worthington, Lakewood, NJ) in PBS for 45 min at 37°C. The resulting cell suspension was filtered, washed, and resuspended in a solution containing monoclonal antibodies (Pharmingen, San Diego, CA) of phycoerythrin-conjugated mouse anti-rat CD31 (1  $\mu\text{g}/\text{million}$  cells) and fluorescein isothiocyanate-conjugated mouse anti-rat CD45 (0.1  $\mu\text{g}/\text{million}$  cells). Cells were then washed and resuspended in 12  $\times$  75 mm polystyrene culture tubes for fluorescence-activated cell sorting analysis. Fluorescence-activated cell sorting analysis was performed on a FACS Vantage SE Cell Sorter (BD Biosciences, San Jose, CA) at the flow cytometry core at the University of Michigan. Cells were gated according to positive fluorescein isothiocyanate and phycoerythrin fluorescence using isotype controls, and the percentage of cells staining positive for each surface antigen was recorded. Similar studies were performed on scaffolds that had been explanted from the rat cranial defect model, although in this case a magnetic cell sorting method was used. A cell suspension from the explanted scaffold was created by digesting the scaffold in 200 U/ml type 2 collagenase, filtered through a 45  $\mu\text{m}$  filter, centrifuged, and resuspended in 4% paraformaldehyde for 10 min. Dynabeads<sup>®</sup> Pan Mouse immunoglobulin G (DynaL Biotech; Brown Deer, WI) were purchased and used in combination with monoclonal antibodies for CD45 and CD31 to sort the cells according to the Dynabead protocol. Quantification of angiogenesis in the tissue that had infiltrated the scaffold was performed according to previously described protocols,<sup>21</sup> and four samples were analyzed/condition and three sections/sample were quantified. Osteogenesis in the cranial defect

experiment was determined by examining hematoxylin and eosin-stained tissue sections, and little to no bone formation was noted in the defects at this time point in any experimental condition, as expected from previous studies.<sup>38</sup>

**Quantification of gene expression in vivo.** Quantification of  $\beta$ -gal activity was used to assess the effectiveness of *in vivo* gene transfer following subcutaneous implantation, at 2, 4, and 8 weeks of implantation as described previously.<sup>39</sup> Quantification of BMP-2 activity within the different cell types explanted from the cranial defect was performed to determine the expression of the delivered DNA. The previously magnetically sorted cells were collected by centrifugation and lysed in Carons lysis buffer. An enzyme-linked immunosorbent assay for human BMP-2 (R&D Systems, Minneapolis, MN) was performed on each lysate following the instructions in the enzyme-linked immunosorbent assay kit.

## ACKNOWLEDGMENTS

Financial support for this work was provided by National Institutes of Health (NIH) grant R37 DE013033. In addition K.W.R was supported by a Tissue Engineering and Regeneration Training grant (NIH/NIDCR DE07057).

## REFERENCES

- Kay, MA, Liu, D and Hoogerbrugge, PM (1997). Gene therapy. *Proc Natl Acad Sci USA* **94**: 12744–12746.
- Orkin, SH and Motulsky, AG (1995). Report and recommendations of the panel to assess the NIH investment in research on gene therapy. <http://www.nih.gov/news/panelrep.html>.
- Cavazzana-Calvo, M, Thrasher, A and Mavilio, F (2004). The future of gene therapy. *Nature* **427**: 779–781.
- Domb, AJ and Levy, MY (1999). Polymers in gene therapy. In: Ottenbrite, RM (ed). *Frontiers in Biomedical Polymer Applications*. Technomic Publishing Company: Lancaster, pp 1–15.
- Godbey, WT, Wu, KK and Mikos, AG (1999). Tracking the intracellular path of poly(ethylenimine)/DNA complexes for gene delivery. *Proc Natl Acad Sci USA* **96**: 5177–5181.
- Remy-Kristensen, A, Clamme, JP, Vuilleumier, C, Kuhry, JG and Mely, Y (2001). Role of endocytosis in the transfection of L929 fibroblasts by polyethylenimine/DNA complexes. *Biochim Biophys Acta* **1514**: 21–32.
- Mellman, I (1996). Endocytosis and molecular sorting. *Annu Rev Cell Dev Biol* **12**: 575–625.
- Raucher, D and Sheetz, MP (1999). Membrane expansion increases endocytosis rate during mitosis. *J Cell Biol* **144**: 497–506.
- Tseng, WC, Haselton, FR and Giorgio, TD (1999). Mitosis enhances transgene expression of plasmid delivered by cationic liposomes. *Biochim Biophys Acta* **1445**: 53–64.
- Buckley-Sturrock, A *et al.* (1989). Differential stimulation of collagenase and chemotactic activity in fibroblasts derived from rat wound repair tissue and human skin by growth factors. *J Cell Physiol* **138**: 70–78.
- Davidson, JM *et al.* (1985). Accelerated wound repair, cell proliferation, and collagen accumulation are produced by a cartilage-derived growth factor. *J Cell Biol* **100**: 1219–1227.
- Stuart, KA *et al.* (2000). Hepatocyte growth factor/scatter factor-induced intracellular signalling. *Int J Exp Pathol* **81**: 17–30.
- Kim, BS and Mooney, DJ (1998). Development of biocompatible synthetic extracellular matrices for tissue engineering. *Trends Biotechnol* **16**: 224–230.
- Huang, YC (2004). *Combined Polymeric Scaffold Delivery of Condensed DNA, Protein, Stem Cells for Bone Tissue Engineering* PhD. Thesis, University of Michigan: Ann Arbor, 250.
- Kong, HJ *et al.* (2005). Non-viral gene delivery regulated by stiffness of cell adhesion substrates. *Nat Mater* **4**: 460–464.
- Sosnowski, BA *et al.* (1996). Targeting DNA to cells with basic fibroblast growth factor (FGF2). *J Biol Chem* **271**: 33647–33653.
- Shea, LD, Smiley, E, Bonadio, J and Mooney, DJ (1999). DNA delivery from polymer matrices for tissue engineering. *Nat Biotechnol* **17**: 551–554.
- Fang, J *et al.* (1996). Stimulation of new bone formation by direct transfer of osteogenic plasmid genes. *Proc Natl Acad Sci USA* **93**: 5753–5758.
- Bonadio, J, Smiley, E, Patil, P and Goldstein, S (1999). Localized, direct plasmid gene delivery *in vivo*: prolonged therapy results in reproducible tissue regeneration. *Nat Med* **5**: 753–759.
- Shida, J, Jingushi, S, Izumi, T, Iwaki, A and Sugioka, Y (1996). Basic fibroblast growth factor stimulates articular cartilage enlargement in young rats *in vivo*. *J Orthop Res* **14**: 265–272.
- Kaigler, D *et al.* (2005). Endothelial cell modulation of bone marrow stromal cell osteogenic potential. *FASEB J* **19**: 665–667.
- Okazaki, H *et al.* (1999). Stimulation of bone formation by recombinant fibroblast growth factor-2 in callotaxis bone lengthening of rabbits. *Calcif Tissue Int* **64**: 542–564.

23. Wang, JS (1996). Basic fibroblast growth factor for stimulation of bone formation in osteoinductive or conductive implants. *Acta Orthop Scand Suppl* **269**: 1–33.
24. Zellin, G and Linde, A (2000). Effects of recombinant human fibroblast growth factor-2 on osteogenic cell populations during orthopic osteogenesis *in vivo*. *Bone* **26**: 161–168.
25. Ono, I, Tateshita, T, Takita, H and Kuboki, Y (1996). Promotion of the osteogenetic activity of recombinant human bone morphogenetic protein by basic fibroblast growth factor. *J Craniofac Surg* **7**: 418–425.
26. Ripamonti, U, Duneas, N, Van Den Heever, B, Bosch, C and Crooks, J (1997). Recombinant transforming growth factor-beta1 induces endochondral bone in the baboon and synergizes with recombinant osteogenic protein-1 (bone morphogenetic protein-7) to initiate rapid bone formation. *J Bone Miner Res* **12**: 1584–1595.
27. Akita, S, Fukui, M, Nakagawa, H, Fujii, T and Akino, K (2004). Cranial bone defect healing is accelerated by mesenchymal stem cells induced by coadministration of bone morphogenetic protein-2 and basic fibroblast growth factor. *Wound Repair Regen* **12**: 252–259.
28. Vonau, RL, Bostrom, MP, Aspenberg, P and Sams, AE (2001). Combination of growth factors inhibits bone ingrowth in the bone harvest chamber. *Clin Orthop Relat Res* **386**: 243–251.
29. Lo, YM *et al.* (1999). Rapid clearance of fetal DNA from maternal plasma. *Am J Hum Genet* **64**: 218–224.
30. Cosio, FG *et al.* (1987). Clearance of human antibody/DNA immune complexes and free DNA from the circulation of the nonhuman primate. *Clin Immunol Immunopathol* **42**: 1–9.
31. Cohen, S, Yoshioka, T, Lucarelli, M, Hwang, LH and Langer, R (1991). Controlled delivery systems for proteins based on poly(lactic/glycolic acid) microspheres. *Pharm Res* **8**: 713–720.
32. Mooney, DJ, Baldwin, DF, Suh, NP, Vacanti, JP and Langer, R (1996). Novel approach to fabricate porous sponges of poly(D,L-lactic-co-glycolic acid) without the use of organic solvents. *Biomaterials* **17**: 1417–1422.
33. Sheridan, MH, Shea, LD, Peters, MC and Mooney, DJ (2000). Bioabsorbable polymer scaffolds for tissue engineering capable of sustained growth factor delivery. *J Control Release* **64**: 91–102.
34. Smith, MK, Peters, MC, Richardson, TP, Garbern, JC and Mooney, DJ (2004). Locally enhanced angiogenesis promotes transplanted cell survival. *Tissue Eng* **10**: 63–71.
35. Smith, MK, Riddle, KW and Mooney, DJ (2006). Delivery of hepatotropic factors fails to enhance longer-term survival of subcutaneously transplanted hepatocytes. *Tissue Eng* **12**: 235–244.
36. Riddle, KW and Mooney, DJ (2004). Role of poly(lactide-co-glycolide) particle size on gas-foamed scaffolds. *J Biomater Sci Polym Ed* **15**: 1561–1570.
37. Murphy, WL, Simmons, CA, Kaigler, D and Mooney, DJ (2004). Bone regeneration via a mineral substrate and induced angiogenesis. *J Dent Res* **83**: 204–210.
38. Huang, YC, Simmons, C, Kaigler, D, Rice, KG and Mooney, DJ (2005). Bone regeneration in a rat cranial defect with delivery of PEI-condensed plasmid DNA encoding for bone morphogenetic protein-4 (BMP-4). *Gene Therapy* **12**: 418–426.
39. Huang, YC, Riddle, K, Rice, KG and Mooney, DJ (2005). Long-term *in vivo* gene expression via delivery of PEI-DNA condensates from porous polymer scaffolds. *Hum Gene Ther* **16**: 609–617.